Specific heat and angle-resolved photoemission spectroscopy study of the superconducting gaps in LiFeAs

U. Stockert,[1,2,*] M. Abdel-Hafiez,[1] D. V. Evtushinsky,[1] V. B. Zabolotnyy,[1] A. U. B. Wolter,[1] S. Wurmehl,[1] I. Morozov,[1,3] R. Klingeler,[4] S. V. Borisenko,[1] and B. Büchner[1]

[1]*Institute for Solid State Research, IFW Dresden, DE-01171 Dresden, Germany*

[2]*MPI for Chemical Physics of Solids, DE-01187 Dresden, Germany*

[3]*Moscow State University, Moscow 119991, Russia*

[4]*Kirchhoff Institute for Physics, University of Heidelberg, DE-69120 Heidelberg, Germany*

(Received 18 November 2010; revised manuscript received 17 February 2011; published 27 June 2011)

We present specific-heat, c_p, and angle-resolved photoemission spectroscopy (ARPES) data on single crystals of the stoichiometric superconductor LiFeAs. A pronounced anomaly is found in c_p at the superconducting transition. The electronic contribution can be described by two s-type energy gaps with magnitudes of approximately $\Delta_1 = 1.2$ meV and $\Delta_2 = 2.6$ meV and a normal-state γ coefficient of 10 mJ/mol K^2. All these values are in agreement with ARPES results.

DOI: 10.1103/PhysRevB.83.224512 PACS number(s): 74.25.Bt, 74.25.Jb, 74.70.Xa

I. INTRODUCTION

The symmetry of the superconducting order parameter is one of the basic characteristics of the superconducting state. In this respect, the recently discovered pristine superconductor LiFeAs with a T_c of approximately 18 K[1–3] plays a decisive role in elucidating the pairing mechanism of the Cooper pairs and the nature of the superconducting state in pnictide superconductors. In contrast to other pnictides, superconductivity in LiFeAs evolves without additional doping, and nesting between hole and electron pockets is very poor.[4] The evolution of spin-density-wave (SDW) type magnetic order, which is typically present in the vicinity of the superconducting state in so-called "1111" and "122" pnictide superconductors, is not observed in LiFeAs. Consequently, mediation of superconductivity by antiferromagnetic spin fluctuations as suggested for other pnictides[5,6] is unlikely. Remarkably, there is evidence both from theory and experiments for almost ferromagnetic fluctuations that drive an instability toward spin-triplet p-wave superconductivity.[7,8]

Experimental investigations on the structure and magnitude of the superconducting gaps in LiFeAs by means of bulk specific-heat data as well as by angle-resolved photoemission spectroscopy (ARPES) are of great interest. Previous specific-heat data obtained on an assembly of tiny LiFeAs single crystals are in agreement with the presence of two isotropic gaps of 0.7 and 2.5 meV, although the presence of nodes could not be ruled out.[9] Similarly, magnetization measurements on polycrystals suggest two s-type gaps of 0.6 and 3.3 meV, but do not exclude gap nodes.[10] Recent magnetization data of single crystals revealed two gaps of approximately 1.3 and 2.9 meV.[11] Measurements of the London penetration depth of single crystals are in line with nodeless superconductivity and two gaps of 1.7 and 2.9 meV.[12,13] ARPES measurements suggest the presence of two gaps of 1.5 and 2.5 meV as well,[4] with the larger one being in reasonable agreement with the results of the data analysis presented in Ref. 14.

In this manuscript, we study the superconducting energy gaps of LiFeAs single crystals by two complementary experimental methods, specific-heat measurements and ARPES. The specific heat is sensitive to the bulk and gives direct access to the entropy of Cooper-pair breaking, which is determined by the superconducting gap structure. In turn, ARPES allows for probing the momentum-resolved superconducting gap. From our results we can exclude the possibility of d-wave pairing in LiFeAs. Instead, both methods are in line with the existence of at least two s-type energy gaps for different Fermi-surface sheets of LiFeAs with magnitudes of approximately $\Delta_1 = 1.2$ meV and $\Delta_2 = 2.6$ meV.

II. EXPERIMENTAL METHODS

Single crystals of LiFeAs have been prepared by a self-flux method described in detail in Ref. 15. Specific-heat data were obtained by a relaxation technique in a physical properties measurement system (PPMS) (Quantum Design) on a sample with a mass of 2.4 mg. Measurements of the magnetic susceptibility in a field of 2 mT (MPMS-XL from Quantum Design) confirmed that this sample has a magnetic T_c^{χ} of 16.9 K, similar to other crystals from the same batch.[15] After correction for demagnetization effects using an ellipsoid approximation for the sample shape, the superconducting volume fraction was estimated to 0.91. The difference to 100% is within the error of demagnetization and may be due to deviations of the sample from an ellipsoid and/or due to a small nonsuperconducting phase. Photoemission experiments have been carried out using the synchrotron radiation from the BESSY storage ring. The end-station "1-cubed ARPES" is equipped with a ^{3}He cryostat which allows to collect angle-resolved spectra at temperatures below 1 K. All single crystals have been cleaved in UHV exposing the mirror-like surfaces.

III. RESULTS

The temperature dependence of the specific heat, c_p, of a LiFeAs single crystal is shown in Fig. 1 as c_p/T versus T. In zero magnetic field a clear anomaly is observed around 15 K, which is attributed to the superconducting phase transition. By

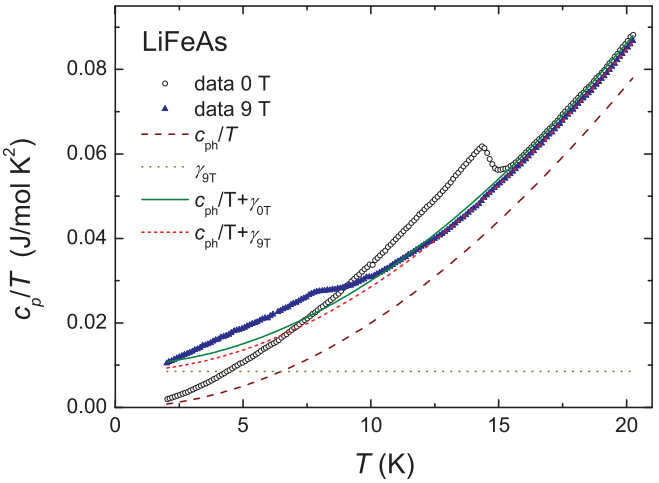

FIG. 1. (Color online) The temperature dependence of the specific heat of LiFeAs is shown as c_p/T vs T in zero magnetic field and in a field $B \parallel c$ of 9 T. The phonon and electron contributions $c_{\rm ph}$ and $c_{\rm el-n\,9T}$ have been determined from a fit of the 9-T data as explained in the text. In addition, the fitted total c_p/T for 0 and 9 T are shown.

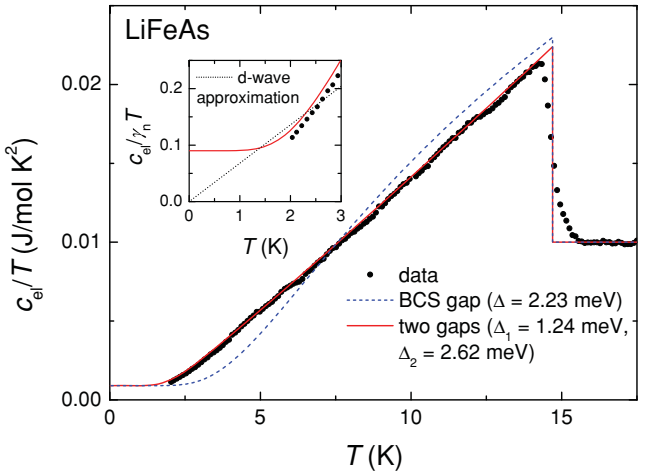

FIG. 2. (Color online) The main plot shows the electronic contribution to the specific heat of LiFeAs in zero field as $c_{\rm el}/T$ vs T. The dotted line corresponds to a single-gap BCS curve taking into account a residual nonsuperconducting contribution with $\gamma_{\rm res}/\gamma_n = 0.09$. The red curve is a two-gap model of the data assuming likewise $\gamma_{\rm res}/\gamma_n = 0.09$. The inset shows the low-T data as $c_{\rm el}/\gamma_n T$ vs T on a larger scale. In addition, an estimate for the low-T $c_{\rm el}$ expected in case of a d-wave order parameter is plotted.

applying a magnetic field $B = \mu_0 H \parallel c$ of 9 T the anomaly is shifted to lower temperatures and reduced in height.

In order to determine the specific heat related to the superconducting phase transition, we need to estimate the phonon ($c_{\rm ph}$) and electron ($c_{\rm el-n}$) contributions to c_p in the normal state. At low T, $c_{\rm el-n}$ behaves linear in T while $c_{\rm ph}$ varies as $c_{\rm ph} \propto T^3$. However, for LiFeAs the onset of superconductivity limits the fitting range toward low T. In order to improve the reliability at higher T, we used a second term of the harmonic-lattice approximation, i.e., $c_{\rm el-n} + c_{\rm ph} = \gamma T + \beta_3 T^3 + \beta_5 T^5$. The results of a fit of the 9-T data between 13 and 20 K are shown as lines in Fig. 1. From the fitting parameters we calculated a Debye temperature of 310 K and a Sommerfeld coefficient of $\gamma_{9\rm T} = 8.5$ mJ/mol K^2. Below 13 K the 9-T data deviate slightly from the fit, although the superconducting transition is observed only around 8 K. This may be due to a tiny part of the sample with different orientation $B \parallel ab$. For this field direction the superconducting transition in 9 T is known to take place at 13 K.[16] The data above 13 K are well described by the fit.

The zero-field specific heat is shifted by a constant with respect to the 9-T curve above T_c, which is attributed to a field-dependent electronic specific heat. From our data we obtain a zero-field Sommerfeld coefficient $\gamma_{0\rm T} = \gamma_n = 10.0$ mJ/mol K. This value is about half the one determined in previous specific-heat studies on polycrystalline LiFeAs[17] and on an assembly of small single crystals.[9] The differing γ coefficient may arise from differences in the sample quality. Resistivity measurements on a crystal from the same batch as the one investigated here revealed a very low residual resistivity of only 15.2 $\mu\Omega$cm and a large residual resistivity ratio, RRR $= \rho_{300\,\rm K}/\rho_{0\,\rm K}$, of 38.[18] This confirms the high quality of our samples. By contrast, the polycrystalline LiFeAs investigated in Ref. 17 exhibits a much larger residual resistivity of approximately 2.5 mΩcm with RRR $\approx$ 10. This may be an indication for the presence of impurities, which can give rise to additional contributions to the specific heat.

Figure 2 shows the temperature dependence of the electronic contribution to the specific heat, $c_{\rm el}$, in zero-field determined by subtracting $c_{\rm ph}$. From an entropy-conserving construction we find a superconducting transition temperature of $T_c = 14.7$ K, which is somewhat smaller than the magnetic T_c^{χ} of the sample. This difference between the thermodynamic and magnetic T_c has been also found in previous studies of LiFeAs.[9,17] Of particular interest in this context is a recent investigation of single-crystalline LiFeAs:[16] the onset value of T_c determined by dc susceptibility in 1 mT was found to be about 17 K. However, the extrapolation of the field dependence, $T_c(B)$, determined by magnetic-torque measurements on a small piece from the same crystal yielded a zero-field T_c of 15.5 K. Likewise, ac-susceptibility data for $B \gtrsim 0.5$ T on crystals from the same batch extrapolate to a lower T_c than the values measured in very small fields. Therefore, the difference between the low-field T_c^{χ} and the bulk T_c determined, e.g., by specific heat, appears inherent to LiFeAs.

The jump height of $c_{\rm el}/T$ at T_c amounts to 1.24 γ_n, which is slightly lower than the BCS value of 1.43γ_n. In addition, the almost linear temperature dependence of $c_{\rm el}/T$ indicates that the specific-heat data cannot be described by a single BCS gap. In order to illustrate this, we show a theoretical BCS curve with $\Delta = 1.764\, k_{\rm B} T_c = 2.23$ meV in Fig. 2, where we account for a small fraction $\gamma_{\rm res}/\gamma_n = 0.09$ of normal electrons as justified below. Systematic deviations of the single-gap fit from the data are observed in the whole temperature range below T_c. Since a single gap cannot describe the data, we applied a phenomenological two-gap model developed for the specific heat of MgB_2.[19] For this purpose we calculated theoretical curves $c_{\rm el}/T$ versus T for a large range of the free parameters Δ_1, Δ_2, $\gamma_{\rm res}$, and the weight of the gaps $w_{\Delta 2/\Delta 1}$.

We then calculated the differences d_i between these curves and the data point by point and used the sum of the squares Σd_i^2 as criteria for the model quality. The best description of the data is obtained for $\Delta_1 = 1.44$ meV, $\Delta_2 = 2.74$ meV, $\gamma_{\rm res}/\gamma_n = 0.13$, and $w_{\Delta 2/\Delta 1} = 1.18$. This result, however, is not realistic: the measured data exclude values larger than 0.11 for $\gamma_{\rm res}/\gamma_n$. This is seen from the inset of Fig. 2, which shows the low-temperature ratio $c_{\rm el}/\gamma_n T$. It reaches a value of 0.11 around 2 K. In view of the systematic decrease of the data with decreasing temperature, it is likely that the ratio $\gamma_{\rm res}/\gamma_n$ is even lower. Therefore, we take the normal-state contribution determined from the magnetic susceptibility of the same sample to estimate $\gamma_{\rm res}/\gamma_n = 0.09$. By doing so, the best description of the data is obtained for $\Delta_1 = 1.24$ meV, $\Delta_2 = 2.62$ meV, and $w_{\Delta 2/\Delta 1} = 1.53$. The corresponding calculated specific heat is shown as a red line in Fig. 2. It is in a very good agreement with the data in the whole temperature range. Still, a close look to the low-T part (cf. inset of Fig. 2) reveals systematic deviations from the data, which suggests an even lower $\gamma_{\rm res}$.

Although the data are best reproduced by the parameters given above, they can be described with similar accuracy for a considerable range of gaps. For an estimate we consider all curves for which the deviation from the data Σd_i^2 is at most 2 times the value for the best curve with $\gamma_{\rm res}/\gamma_n = 0.09$. As an additional constraint we assume $\gamma_{\rm res}/\gamma_n \leqslant 0.11$ in agreement with the data. Thus, we obtain $\Delta_1 = (0.93$–$1.67)$ meV, $\Delta_2 = (2.40$–$3.24)$ meV, $\gamma_{\rm res}/\gamma_n = 0.04$–$0.11$, and $w_{\Delta 2/\Delta 1} = 0.46$–$3.45$.

The overall shape of the superconducting anomaly presented here is similar to the one obtained recently on a cluster of tiny single crystals of LiFeAs.[9] However, the magnitudes of the gaps are somewhat larger, in particular for the smaller gap of 1.24 meV compared to 0.7 meV obtained in Ref. 9. This may be due to the limited resolution of the data in Ref. 9, which leaves a considerable uncertainty for $\gamma_{\rm res}$. In addition, the magnitude of the smaller gap Δ_1 itself is very sensitive to the specific heat at low T. The high resolution of our data down to 2 K allows for a very reliable estimate of both $\gamma_{\rm res}$ and Δ_1. In Ref. 9, even a d-wave order parameter could not be ruled out. In this case, one should find a linear-in-T behavior of $c_{\rm el}/T$ for $T \ll T_c$. Since our measurement range is limited to $T > 0.14\ T_c$, we cannot directly exclude the presence of line-nodes of the gap function either. However, the quality of our data and the low value at 2 K render the presence of line nodes of the gap function very unlikely. This is demonstrated by the expected low-T behavior for a d-wave order parameter estimated as described in Ref. 9 and assuming $\gamma_{\rm res} = 0$. It cannot be brought into an agreement with the measured data. Taking into account, in addition, recent ARPES results suggesting a nearly isotropic gap for each Fermi-surface sheet,[4] a d-wave order parameter is excluded from the consideration.

Owing to its ability to resolve both momentum and energy of the electronic states, ARPES can provide a complete picture of the electronic band dispersion and the momentum-dependent superconducting gap. Therefore, it is interesting to compare the thermodynamic properties measured directly with those calculated from photoemission data. In particular, one can quite easily extract the value of the Sommerfeld coefficient γ_n. This parameter determines the heat capacity in the normal state, and, along with the superconducting-gap values and the assumption of BCS pairing, the thermodynamic properties in the superconducting state. For this purpose the photoemission intensity of the LiFeAs has been mapped in more than one Brillouin zone (BZ) and fitted with the standard tight-binding formula.[20,21] To demonstrate the agreement between the ARPES raw data and the obtained tight-binding fits, in Figs. 3(a) and 3(b), we show two high-symmetry cuts along Γ-X-Γ and Γ-M-Γ directions with the fits to the renormalized quasiparticle dispersions superimposed over the ARPES data. As one may see from the derived density of states (DOS) [see Fig. 3(c)], the major contribution to the heat capacity must be due to the outer hole band. Another interesting observation is a quite pronounced variation in the DOS at the Fermi level, which may result in deviations from the linear temperature dependence of the electronic heat capacity. To check to which extent this applies to the current case, instead of using a standard textbook expression for the electronic heat capacity $c_{\rm el} \propto \mathcal{D}(E_{\rm F}) k_{\rm B} T$, we have made an estimate based on a more general expression, which for a single quasiparticle band with dispersion $\mathcal{E}_{k_i}$ reads as $c_M = 2N_{\rm A} \frac{\partial}{\partial T} \langle f(\mathcal{E}_{k_i}, T) \mathcal{E}_{k_i} \rangle_{\rm BZ}$. Here, $\langle \cdots \rangle_{\rm BZ}$ denotes an average over the Brillouin zone and $N_{\rm A}$ is the Avogadro constant. Indeed, the value of $\mathrm{d}c_{\rm el}/\mathrm{d}T$, that in case of strict temperature linearity defines the Sommerfeld coefficient γ_n, varies from 13 to about 17 mJ/mol K^2, which is in a relatively good agreement with the direct measurements resulting in $\gamma_n \approx 10$ mJ/mol K^2. This variation in the $dc_{\rm el}/dT$ is also likely to account for some variation in the γ_n extracted from the thermodynamic measurements by different authors.

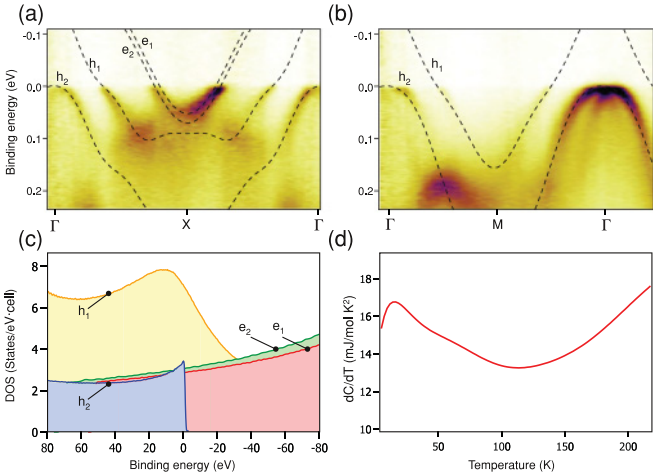

FIG. 3. (Color online) (a) and (b) Photoemission intensity in the high-symmetry cuts together with the fitted tight-binding dispersions. e_1 and e_2 are the two bands forming the electron pockets at the X point of the BZ. h_1 and h_2 are the outer and the inner hole bands centered at the Γ point. (c) Band contribution to the DOS derived from the fitted quasiparticle dispersions. (d) Temperature-dependent Sommerfeld coefficient determined as $\gamma(T) = dc_{\rm el}/dT$.

Next we address the issue of the temperature dependence of the superconducting gap on the basis of spectroscopic data. Figure 4(a) shows integrated energy distribution curves (IEDCs), which were obtained from photoemission spectra recorded at different temperatures. Integration was performed for the momentum region of the electron-like barrel around the M point. Upon cooling through T_c, a peak appears near

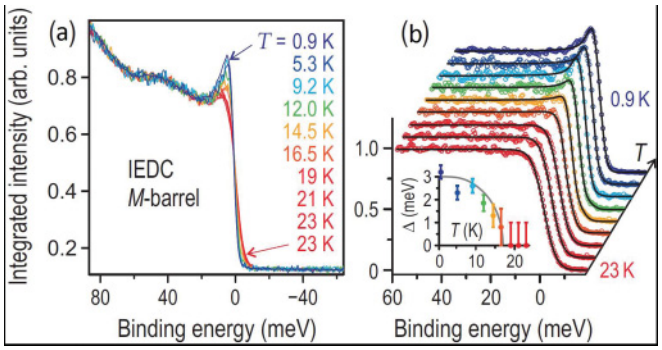

FIG. 4. (Color online) (a) Integrated energy distribution curves (IEDCs) for the electron-like M barrel, measured in the temperature range from 0.9 to 23 K. (b) Normalized IEDCs with fits to the Dynes function. Inset: derived temperature dependence of the superconducting gap.

the Fermi level in the IEDCs, which grows with decreasing temperature. It indicates the opening of the superconducting gap in the DOS of the M barrel and the formation of the Bogoliubov quasiparticle dispersion. To derive the temperature dependence of the gap, we normalized the IEDCs to the data taken above T_c (at 23 K) and fitted them to the Dynes function[22] [see Fig. 4(b)]. The result of this procedure is plotted in the inset of Fig. 4(b). First indications for the presence of the gap are observed close to T_c. Below T_c, the gap magnitude follows the BCS temperature dependence with $\Delta(T \to 0) = 3$ meV within the experimental error bars. This is in agreement with our specific-heat results suggesting the presence of two *s*-type gaps with BCS temperature dependence in LiFeAs.

It is remarkable that the thermodynamic-gap values determined in the present study are in excellent agreement with the ARPES leading-edge gaps reported in Ref. 4 (1.5 and 2.5 meV). However, the absolute values of the actual gaps, which can be derived from the ARPES data after a more rigorous analysis, are usually slightly higher than the leading-edge ones. The resulting discrepancy (of the order of 0.5 meV) between the absolute gap values derived from ARPES and in the present study could probably be explained by the difference in thermodynamic and magnetic T_c mentioned before. In any case, the ratio of the ARPES leading-edge gaps reproduces the ratio of the actual gap values quite accurately, and this is in close correspondence with the ones discussed here. Moreover, a more detailed investigation of the superconducting gaps in LiFeAs[23] indicates that the value of the gap supported by the band h2 is indeed comparable to that of the large hole Fermi surface, made by the band h1 [see Fig. 3(a)]. In the light of the results presented in Fig. 3(c), it is important to establish the fact that the smaller gap corresponds to the hole-like Fermi surfaces centered around the Gamma point while the larger one corresponds to the electron-like Fermi surfaces localized around the corners of the Brillouin zone. This knowledge can help to identify the symmetry of the order parameter in iron pnictides in more details.

IV. SUMMARY

In summary, both thermodynamic and spectroscopic experiments on LiFeAs render a nodal gap very unlikely, and, equivocally speaking, are in favor of a strong variation of the gap magnitude between different electronic bands, from about 1.2 to 2.6 meV. The general agreement of such complementary probes within band picture emphasizes the robustness of the conclusions drawn. The multigap behavior of LiFeAs established above is in line with two gaps found in many other iron arsenides.

ACKNOWLEDGMENTS

We thank D. Inosov for useful discussions. Work was supported by the Deutsche Forschungsgemeinschaft through the Priority Program SPP1458 (BE1749/13). I.M. acknowledges support from the Ministry of Science and Education of the Russian Federation under State contract P-279 and by RFBR-DFG (Project No. 10-03-91334).

*ulrike.stockert@cpfs.mpg.de

[1] J. H. Tapp, Z. Tang, B. Lv, K. Sasmal, B. Lorenz, P. C. W. Chu, and A. M. Guloy, Phys. Rev. B **78**, 060505(R) (2008).
[2] M. J. Pitcher, D. R. Parker, P. Adamson, S. J. C. Herkelrath, A. T. Boothroyd, and S. J. Clarke, Chem. Commun. **2008**, 5918 (2008).
[3] X. C. Wang, Q. Q. Liu, Y. X. Lv, W. B. Gao, L. X. Yang, R. C. Yu, F. Y. Li, and C. Q. Jin, Solid State Commun. **148**, 538 (2008).
[4] S. V. Borisenko, V. B. Zabolotnyy, D. V. Evtushinsky, T. K. Kim, I. V. Morozov, A. N. Yaresko, A. A. Kordyuk, G. Behr, A. Vasiliev, R. Follath, and B. Büchner, Phys. Rev. Lett. **105**, 067002 (2010).
[5] K. Kuroki, S. Onari, R. Arita, H. Usui, Y. Tanaka, H. Kontani, and H. Aoki, Phys. Rev. Lett. **101**, 087004 (2008).
[6] I. I. Mazin, D. J. Singh, M. D. Johannes, and M. H. Du, Phys. Rev. Lett. **101**, 057003 (2008).
[7] P. M. R. Brydon, M. Daghofer, C. Timm, and J. van den Brink, Phys. Rev. B **83**, 060501(R) (2011).
[8] S.-H. Baek *et al.* (unpublished).
[9] F. Wei, F. Chen, K. Sasmal, B. Lv, Z. J. Tang, Y. Y. Xue, A. M. Guloy, and C. W. Chu, Phys. Rev. B **81**, 134527 (2010).
[10] K. Sasmal, B. Lv, Z. Tang, F. Y. Wei, Y. Y. Xue, A. M. Guloy, and C. W. Chu, Phys. Rev. B **81**, 144512 (2010).
[11] Y. J. Song, J. S. Ghim, J. H. Yoon, K. J. Lee, M. H. Jung, H.-S. Ji, J. H. Shim, and Y. S. Kwon, EPL **94**, 57008 (2011).
[12] H. Kim, M. A. Tanatar, Y. J. Song, Y. S. Kwon, and R. Prozorov, e-print arXiv:1008.3251 (unpublished).
[13] Y. Imai, H. Takahashi, K. Kitagawa, K. Matsubayashi, N. Nakai, Y. Nagai, Y. Uwatoko, M. Machida, and A. Maeda, J. Phys. Soc. Jpn. **80**, 013704 (2011).
[14] D. S. Inosov, J. S. White, D. V. Evtushinsky, I. V. Morozov, A. Cameron, U. Stockert, V. B. Zabolotnyy, T. K. Kim, S. V. Borisenko, E. M. Forgan, R. Klingeler, J. T. Park, S. Wurmehl, A. N. Vasiliev, G. Behr, C. D. Dewhurst, and V. Hinkov, Phys. Rev. Lett. **104**, 187001 (2010).

[15]I. Morozov, A. Boltalin, O. Volkova, A. Vasiliev, O. Kataeva, U. Stockert, M. Abdel-Hafiez, D. Bombor, A. Bachmann, L. Harnage, M. Fuchs, H.-J. Grafe, G. Behr, R. Klingeler, S. Borisenko, C. Hess, S. Wurmehl, and B. Büchner, Crystal Growth and Design **10**, 4429 (2010).

[16]N. Kurita, K. Kitagawa, K. Matsubayashi, A. Kismarahardja, E. S. Choi, J. S. Brooks, Y. Uwatoko, and S. Uji, T. Terashima. J. Phys. Soc. Jpn. **80**, 013706 (2011).

[17]C. W. Chu, F. Chen, M. Gooch, A. M. Guloy, B. Lorenz, B. Lv, K. Sasmal, Z. J. Tang, J. H. Tapp, and Y. Y. Xue, Physica C **469**, 326 (2009).

[18]O. Heyer, T. Lorenz, V. B. Zabolotnyy, D. V. Evtushinsky, S. V. Borisenko, I. Morozov, L. Harnagea, S. Wurmehl, C. Hess, B. Büchner, e-print arXiv:1010.2876 (unpublished).

[19]F. Bouquet, Y. Wang, R. A. Fisher, D. G. Hinks, J. D. Jorgensen, A. Junod, and N. E. Phillips, Europhys. Lett. **56**, 856 (2001).

[20]A. A. Kordyuk, S. V. Borisenko, M. Knupfer, and J. Fink, Phys. Rev. B **67**, 064504 (2003).

[21]D. S. Inosov, V. B. Zabolotnyy, D. V. Evtushinsky, A. A. Kordyuk, B. Büchner, R. Follath, H. Berger, and S. V. Borisenko, New J. Phys. **10**, 125027 (2008).

[22]D. V. Evtushinsky, D. S. Inosov, V. B. Zabolotnyy, M. S. Viazovska, R. Khasanov, A. Amato, H.-H. Klauss, H. Luetkens, C. Niedermayer, G. L. Sun, V. Hinkov, C. T. Lin, A. Varykhalov, A. Koitzsch, M. Knupfer, B. Büchner, A. A. Kordyuk, and S. V. Borisenko, New J. Phys. **11**, 055069 (2009).

[23]S. V. Borisenko (unpublished).